THE JOURNAL OF PHYSICAL CHEMISTRY B

Article

pubs.acs.org/JPCB

Comparison of Aggregation Behaviors of a Phytosterol Ethoxylate Surfactant in Protic and Aprotic Ionic Liquids

Xiu Yue, Xiao Chen,* and Qintang Li

Key Laboratory of Colloid and Interface Chemistry, Shandong University, Ministry of Education, Jinan, 250100, China

ABSTRACT: Two different room-temperature ionic liquids (ILs), the protic ethylammonium nitrate (EAN) and the aprotic 1-butyl-3-methylimidazolium tetrafluoroborate ([Bmim]BF_4), have been employed to investigate the solvent protonation effect on aggregation behaviors of a phytosterol ethoxylate surfactant (BPS-10). The calculated thermodynamic parameters based on surface tension measurements present a stronger solvophobic interaction in EAN than that in [Bmim]BF_4 and disclose different driving forces for micelle formation. In addition, the polarized optical microscopy and small-angle X-ray scattering techniques are used to characterize the phase structures formed in both systems at 25 °C. Due to the H-bonding networks in protic EAN, BPS-10 exhibits a lyotropic liquid-crystalline behavior different from that in [Bmim]BF_4. Results obtained from the rheological measurements reflect a more viscoelastic nature of lyotropic liquid-crystalline phases in EAN. The obtained results indicate that the protic EAN behaves more effective than [Bmim]BF_4 to promote the nonionic BPS-10 aggregation.

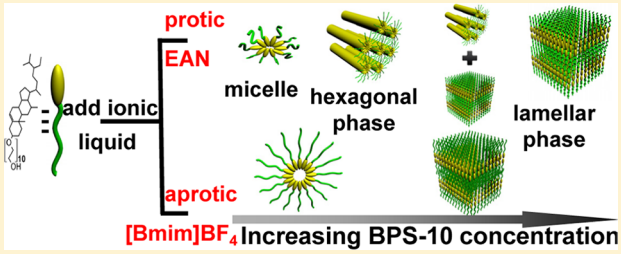

INTRODUCTION

Ionic liquids (ILs), as a novel-type organic solvent, have attracted scientists' attention for their synthesis,[1] catalysis,[2−4] electrochemistry,[5,6] and other applications due to their special physicochemical properties. On the view of colloid and surface chemistry, the most unique capability of ILs, including the protic (PILs) and the aprotic (AILs), is to play a part as new media for the self-assembled structures of surfactants.[7,8] The main difference between these two classes of ILs is the capability of donating and accepting protons. The former can thus build up hydrogen-bonding networks similar to water, whereas the later cannot.[8,9] Up to now, many alkylammonium-type PILs, such as ethylammonium nitrate (EAN), and a small number of AILs represented by imidazolium salts have been used as solvents for amphiphile self-assembly. Among them, the aggregations of nonionic surfactants are widely investigated, where the solvophobic interactions are dominated. Patrascu et al.[10] reported that the alkyl poly(ethylene glycol) ethers (C_nE_m) could form micelles in 1-butyl-3-methylimidazolium (Bmim) AILs with different counterions (BF_4^-, PF_6^-, Tf_2N^-). The micelle sizes and the aggregation numbers have close relationships with the anion species of the ILs. After that, on the basis of the temperature dependence of the critical micelle concentration (CMC), Inoue et al.[11,12] evaluated the thermodynamic parameters and the solvophobic interaction between hydrocarbon chains for micelle formation of C_nE_m in [Bmim]BF_4. The self-assembled structures of a series of nonionic surfactants in EAN and other PILs at higher concentrations, however, were studied by Warr's group.[13−16] Meanwhile, we have also investigated several systems with nonionic amphiphiles in PIL and AIL.[17−19] The nonaqueous lyotropic liquid-crystalline (LLC) phase of a triblock copolymer P123 ($EO_{20}PO_{70}EO_{20}$) can be formed in [Bmim]PF_6, which acts not only as a solvent but also as a cosurfactant and salt to promote the aggregation.[19] Compared to its phase behavior in water and [Bmim]PF_6, P123 can form an additional reverse bicontinuous cubic phase in EAN.[18]

As the environmentally friendly surfactants, the ethoxylated sterols exhibit amphiphilicity by the hydrophobic steroid nucleus and the hydrophilic polyoxyethylene chain.[20] Such unusual amphiphilic structures lead them to show a unique phase behavior and have caught many scientists' eyes for their physicochemical properties. Their excellent surface activities in water and [Bmim]PF_6 as represented by significant lower CMCs and surface tensions have been observed by Folmer et al.[20] and Sakai et al.[21] Various LLC structures, such as lamellar, cubic, and hexagonal phases, were characterized in these binary systems. We have also recently found their LLC formation in [Bmim]BF_4,[22] where the phase behaviors of four phytosterol etoxylates surfactants with different oxyethylene units have been studied. The solvophobic interaction combined with the hydrogen bonding are proved to be the main driving forces for the LLC phase formation. Considering the wide potential applications of phytosterol ethoxylates, a systematic investigation for solvent effects on their self-assembly in ILs is needed.

On the basis of this motivation, the alkylammonium PILs, EAN, and the imidazolium AILs, [Bmim]BF_4 are employed here as solvents to explore their effects on aggregation behaviors of a ethoxylated phytosterol surfactant (BPS-10) with its chemical structure given in Scheme 1. As an extension of our previous work, both the micelle and the LLC formation

Received: May 29, 2012
Revised: July 15, 2012
Published: July 15, 2012

Scheme 1. Chemical Structure of the Employed Ethoxylated Phytosterol Surfactant

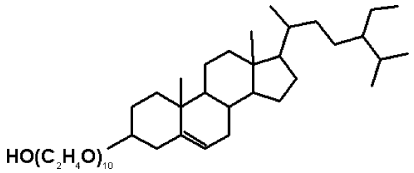

of BPS-10 in two ILs have been investigated. Different LLC phase behaviors and rheological properties have reflected the difference between intermolecular actions in the two solvents. The obtained results should contribute to a better understanding of the solvophobic interaction difference between steroid groups in these two different ILs.

EXPERIMENTAL SECTION

Materials. The room-temperature IL [Bmim]BF_4 (≥99.0%) was purchased from Center for Green Chemistry and Catalysis, LICP, CAS. The ethoxylated phytosterol surfactant BPS-10, where 10 is the number of oxyethylene units, was a kindly supplied gift by Nikkol from Japan. Both were used without further purification. EAN was synthesized according to the procedure described by Evans et al.[23,24] A portion of ~3 M nitric acid was slowly added to the ethylamine solution while stirring and cooling in an ice bath. Water in the resulting solution was removed first with a rotary evaporator and then with a lyophilizer. EAN was freshly synthesized before it was used.

Sample Preparation and Phase Diagram. The BPS-10 surfactant was added to ILs at different mass ratios. The mixtures were heated at 100 °C until the solution became completely transparent without any undissolved ingredient and then homogenized by repeat mixing and centrifugation. Then, the solutions were cooled to room temperature. The samples studied for phase behavior were kept at 25 °C for at least 1 month before further examination. Phase change was determined by ocular observation and visual inspection through crossed polarizers. Accurate determination of the phase boundaries was given by the small-angle X-ray scattering measurement.

Characterization. Surface tension measurements were performed on a KYOWR Interface Science's automatic tensiometer CBVP-A2 using the Wilhelmy plate method. The uncertainty of the surface tension measurements was ±0.2 $mN·m^{-1}$. Temperatures were controlled by a super constant temperature trough with an accuracy of ±0.1 °C. All measurements were repeated at least twice until the values were reproducible. The texture types of the formed LLC phases were taken by a Motic B2 POM with a CCD camera (Panasonic Super Dynamic II WV-CP460). The structural characterizations of LLC phases were performed using an HMBG-SAX X-ray small-angle scattering (SAXS) system (Austria) with Ni-filtered Cu Kα radiation (0.154 nm) operating at 50 kV and 40 mA. The distance from the samples to the detector was 277 mm. The rheology properties were measured on a Haake RS75 stress-controlled rheometer using a cone−plate geometry (C20/1°, Ti). The distance of the cone plates was adjusted to 52 μm. The oscillatory experiments were carried out to determine the viscoelasticities of all samples within the linear viscoelastic region. The sizes of micelles in ILs were measured by dynamic light scattering (DLS) using a Malvern Zetasizer Nano (U.K.). The viscosity (η) and refractive index (n) values of ILs are necessary for DLS measurements. Here, η = 28 cP at 25 °C and n = 1.45 for EAN, and η = 96 cP at 25 °C and n = 1.52 for [Bmim]BF_4. Except as noted, the temperature of the measurements was kept at 25.0 ± 0.1 °C.

RESULTS AND DISCUSSION

The surface tension experiment is often employed to study the adsorption of surfactants at the air−liquid interface and micelle formation. The interfacial properties of the solution and thermodynamic parameters for micelle formation can be derived. It is therefore adopted as a useful tool to investigate the solvent effect of ILs.

Surface Tension Measurements. Surface tension (γ) profiles of the BPS-10 concentrations in EAN and [Bmim]BF_4 were measured to explore their aggregation behaviors. The obtained results are presented in Figure 1. It can be seen that

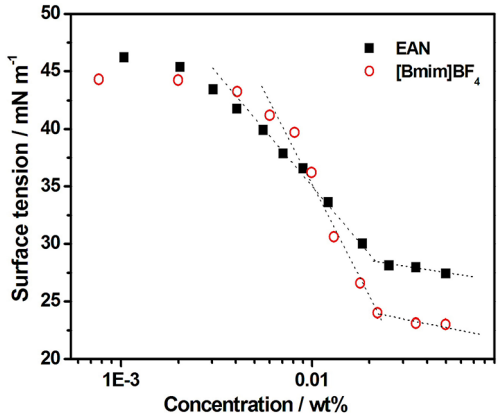

Figure 1. Surface tension profiles of BPS-10 in EAN and [Bmim]BF_4 at 25 °C.

the γ values of both BPS-10/IL systems present an initial gradual decrease with increasing surfactant concentration. Abrupt slope changes of the γ curves follow. After the breaking point, the surface tension becomes more or less constant. Such a γ change suggests the formation of micelles both in EAN and [Bmim]BF_4, which is similar to the conventional nonionic surfactant in ILs[10] or BPS-n in water.[20] However, the derived CMC values (~300 μM) are nearly 2 orders of magnitude higher than that in the aqueous system (~10 μM),[20] which is due to the reduced solvophobic effect in ILs. Meanwhile, the CMCs of BPS-10 in both ILs are approximately the same, with a little higher value in the [Bmim]BF_4 system.

To confirm the micelle formation of BPS-10 in ILs, DLS measurements were performed to characterize the size of self-assembled micelles, with the results shown in Figure 2. The average radii for micelles in EAN and [Bmim]BF_4 systems are 14.1 and 52.8 nm, respectively. The obviously smaller size of micelles in EAN indicates more compact packing of BPS-10 molecules, which is caused by the stronger solvophobic interaction among the sterol groups in EAN. Usually, the radii of micelles formed by conventional nonionic surfactants in EAN are smaller than those for micelles formed in [Bmim]-BF_4,[12,14] indicating different surfactant conformations and interactions with solvents in these two ILs. Hence, we adopt a model for all micelles to comprise a core of sterol groups surrounded by a shell of ethoxy chains. As mentioned above,

dx.doi.org/10.1021/jp305230r | J. Phys. Chem. B 2012, 116, 9439−9444

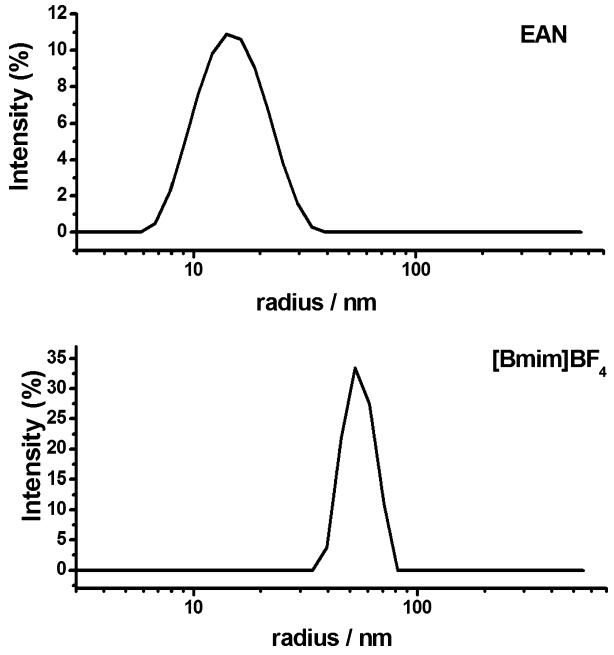

Figure 2. Size distribution of the aggregates formed by BPS-10 in EAN and $[Bmim]BF_4$ at concentrations (wt %) of 4.76×10^{-2} and 4.79×10^{-2}, respectively.

the closer packing of sterol groups and the more coiled ethoxy chains might both make the micelles smaller in EAN. Moreover, the H-bonding between EAN and ethoxy chains will incorporate EAN molecules into the surroundings of ethoxy head groups[14] and lead to a relatively less solvated micelle size. However, such an effect is not so strong in solvent of $[Bmim]BF_4$ due to the weak interaction between $[Bmim]BF_4$ and head groups and the larger $[Bmim]BF_4$ molecular structure.

Several surface parameters are calculated from the γ data and are shown in Table 1. The effectiveness of γ reduction (Π_{CMC}),

Table 1. Surface Properties of BPS-10 in ILs at 25 °C

	CMC (wt %)	γ_{CMC} (mN/m)	Π_{CMC} (mN/m)	Γ_{max} (μmol/m^2)	A_{min} (nm^2)
EAN	2.13×10^{-2}	28.5	20.8	3.3	0.50
$[Bmim]BF_4$	2.28×10^{-2}	24.0	20.2	6.0	0.27

the surface excess at the air/IL interface (Γ_{max}), and the minimum area per surfactant molecule adsorbed at the air/IL interface (A_{min}) can be obtained using the following equations:

$$\Pi_{CMC} = \gamma_0 - \gamma_{CMC} \quad (1)$$

$$\Gamma_{max} = -\frac{d\gamma}{RT\ d \ln CMC} \quad (2)$$

$$A_{min} = \frac{1}{N_A \Gamma_{max}} \quad (3)$$

where γ_0 and γ_{CMC} are, respectively, the surface tensions of pure solvent and the solution at CMC. T is the absolute temperature, N_A is Avogadro's number, and R is the gas constant. From Table 1, it can be found that a much smaller A_{min} occurs in $[Bmim]BF_4$, only approximately half of that in EAN, suggesting that the polyoxyethlene chains are more extended in $[Bmim]BF_4$ but more curved in EAN. The stronger solvophobic interaction between the polyoxyethlene chains and solvent is therefore speculated in EAN because the coiled chain conformation could reduce the contact area with EAN.[25]

The CMC values of BPS-10 in two IL solutions are plotted in Figure 3 as a function of temperature. It is clear that they both

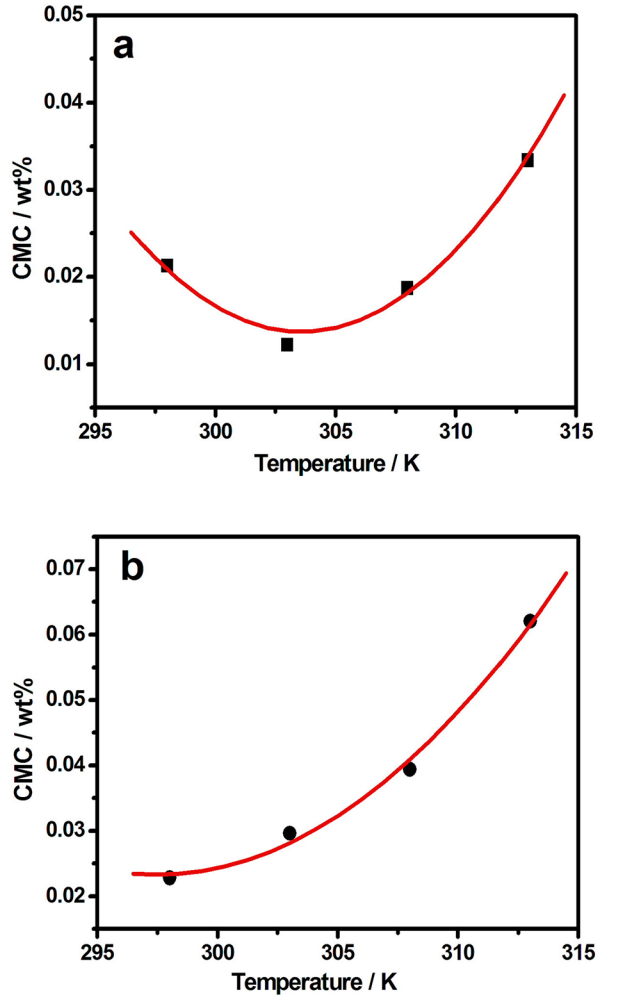

Figure 3. CMC values of BPS-10 in (a) EAN and (b) $[Bmim]BF_4$ solutions as a function of temperature. The solid line is a curve using a second-order polynomial fit.

fit on a U-shaped curve but with different temperatures for minimum CMC. Minimum CMCs appear at 303−308 K in EAN and at around room temperature in $[Bmim]BF_4$.

Such U-shaped CMC versus temperature curves are similar to those observed for other nonionic surfactants in ILs and aqueous solutions,[11] which indicates the solvophobic effect as a dominant driving force for micelle formation. The similar temperature dependence of CMC in both systems suggests an analogous mechanism of micelle formation in EAN and $[Bmim]BF_4$. The difference of temperature for the minimum CMC can be attributed to different strengths of solvophobic interaction between BPS-10 molecules in EAN and $[Bmim]BF_4$. Further information will be discussed in the following part.

Thermodynamic Parameters for Micelle Formation of BPS-10. The micellization of nonionic surfactants can be described with the mass action law model, which assumes equilibrium between the monomer and micelles.[26,27] According

dx.doi.org/10.1021/jp305230r | J. Phys. Chem. B 2012, 116, 9439−9444

to this model, the standard free energy, ΔG_m^0, of micelle formation is given by eq 4.[11,12,26,27]

$$\Delta G_m^0 = RT \ln(X_{cmc}) \quad (4)$$

where X_{cmc} is the CMC expressed in mole fraction units. Once the ΔG_m^0 values are obtained, the standard enthalpy change for micelle formation, ΔH_m^0, can be derived through the Gibbs–Helmholtz equation.

$$\frac{\partial(\Delta G_m^0/T)}{\partial(1/T)} = \Delta H_m^0 \quad (5)$$

Using the acquired ΔG_m^0 and ΔH_m^0 values, the standard entropy change for micelle formation, ΔS_m^0, is calculated by the following equation:

$$\Delta S_m^0 = \frac{\Delta H_m^0 - \Delta G_m^0}{T} \quad (6)$$

On the basis of eqs 4–6, the thermodynamic parameters of micelle formation for two systems are obtained and summarized in Table 1. The plots of these data as a function of temperature for BPS-10 in two ILs are shown in Figure 4, where $-T\Delta S_m^0$ is plotted instead of ΔS_m^0 to make clear the contribution of the entropy term to the free-energy gain associated with the micelle formation. It can be seen that the two plots exhibit certain similarities. The temperature dependence of ΔG_m^0 is rather weak, and ΔH_m^0 decreases with temperature, while $T\Delta S_m^0$ is not. Such variations with temperature are common to other types of surfactants in ILs and aqueous solutions, which are considered as a reflection of the solvophobic interaction between the surfactant molecules.[11,28] However, there is an obvious difference between these two systems. From Table 2, we can find that the driving force of micelle formation in EAN originates from the positive entropy changes at low temperatures and from the negative enthalpy change at high temperatures. However, in the [Bmim]BF_4 system, the enthalpy term is always the main contribution to a negative ΔG_m^0, even at room temperature. What's more, the absolute values of $-T\Delta S_m^0$ for EAN are larger than those for [Bmim]BF_4, indicating a stronger solvophobic interaction in EAN.

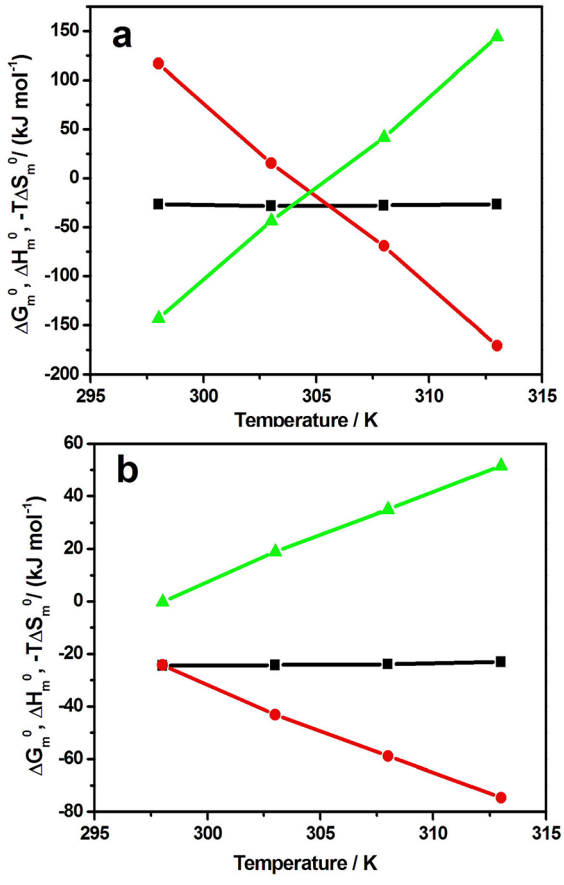

Figure 4. Temperature dependence of thermodynamic parameters for micelle formation of BPS-10 in (a) EAN and (b) [Bmim]BF4. Solid squares, circles, and triangles correspond to ΔG_m^0, ΔH_m^0, and $-T\Delta S_m^0$, respectively.

As mentioned above, the similar trends of the CMC and thermodynamic parameters with increasing temperature indicate an analogous mechanism of micelle formations in EAN and [Bmim]BF_4. The ordered structure by solvent molecules around the solvophobic sterol ring group is deemed to be an origin for the self-assembly of surfactants. Upon micelle formation, such a highly ordered solvent structure is eliminated to release the solvent molecules, which causes the entropy increase and the free-energy decrease. Thus, the larger entropy term for EAN indicates more ordered EAN molecules around the solvophobic sterol ring group. It is attributed to the hydrogen-bond network formed in EAN, but less in [Bmim]-BF_4. Thus, it becomes easy to understand the higher CMC value in [Bmim]BF_4 than that in the EAN system, as shown in Table 2. The ΔS_m^0 value in the EAN system is much higher at the room temperature, while the CMC values of BPS-10 in both ILs are approximately the same, with the one in [Bmim]BF_4 a little higher. This phenomenon is attributed to the interaction of EAN with the ethylene oxide units. As reported previously,[29] the ability to form multiple H-bonding interactions may lead to the enhanced solubility of BPS-10 in EAN.

Phase Behavior of BPS-10 in Two ILs. To further compare the solvent effects, the LLC phase behaviors of BPS-10 in binary systems with EAN and [Bmim]BF_4 have also been investigated by POM and SAXS measurements, with the results shown in Figure 5. Two LLC phases, including the lamellar and the hexagonal, have been disclosed. On the basis of the SAXS results (Figure 5), the lamellar repeat distance d is calculated as 7.46 nm for an 80% BPS-10 concentration in EAN, smaller than 8.10 nm in [Bmim]BF_4 obtained in our previous work.[22] Such a contracted periodicity in EAN reflects again the facts that the stronger solvophobic interaction make BPS-10 packing closer in EAN and the polyoxyethlene chains not so extended as that in [Bmim]BF_4.

As shown in Figure 6 of their phase diagrams, the gradual phase transition for the BPS-10/EAN system goes through from the pure hexagonal LLC (H1) to the coexistence area of H1 and the lamellar phase (Lα) and to Lα phase. However, only the Lα phase was observed at high BPS-10 concentrations in [Bmim]BF_4. It is noted also from Figure 6 that all of the phase structures found in the BPS-10/[Bmim]BF_4 system are maintained in EAN, and the threshold of BPS-10/EAN to form the ordered assembly is at a concentration of 40 wt %, lower than that in [Bmim]BF_4. In other words, the aggregation of BPS-10 molecules to an ordered assembly becomes easier in EAN than that in [Bmim]BF_4 due to the weaker solvophobic interaction in [Bmim]BF_4 than that in EAN, as mentioned above. In addition, the H-bonding can also play a role in the

dx.doi.org/10.1021/jp305230r | J. Phys. Chem. B 2012, 116, 9439–9444

Table 2. CMC and Thermodynamic Parameters of Micelle Formation for BPS-10 in EAN or [Bmim]BF_4 Solution

system	temperature (K)	CMC (wt %)	CMC (mol dm^{-3})	ΔG_m^0 (kJ mol^{-1})	ΔH_m^0 (kJ mol^{-1})	ΔS_m^0 (kJ mol^{-1} K^{-1})
EAN	298	2.13×10^{-2}	2.76×10^{-4}	−26.47	116.67	0.48
EAN	303	1.22×10^{-2}	1.58×10^{-4}	−28.31	15.29	0.14
EAN	308	1.87×10^{-2}	2.42×10^{-4}	−27.69	−69.19	−0.13
EAN	313	3.34×10^{-2}	4.33×10^{-4}	−26.63	−170.57	−0.46
[Bmim]BF_4	298	2.28×10^{-2}	2.86×10^{-4}	−24.47	−24.27	0.0006
[Bmim]BF_4	303	2.96×10^{-2}	3.72×10^{-4}	−24.22	−43.15	−0.06
[Bmim]BF_4	308	3.94×10^{-2}	4.95×10^{-4}	−23.89	−58.89	−0.11
[Bmim]BF_4	313	6.21×10^{-2}	7.80×10^{-4}	−23.09	−74.63	−0.16

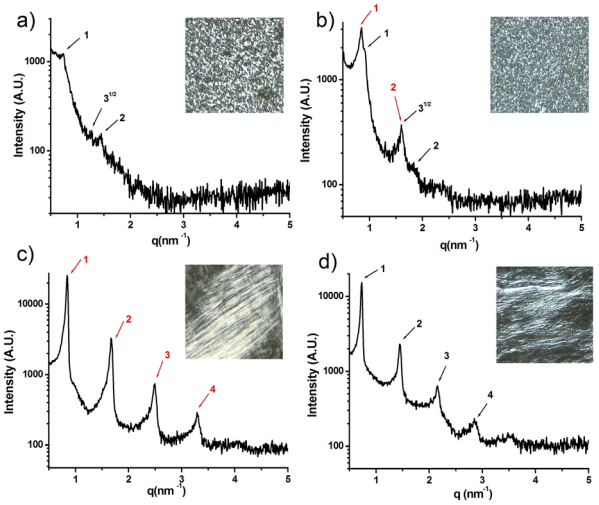

Figure 5. Polarized optical micrographs (inset) and SAXS patterns at room temperature for the anisotropic LLC mesophases with different concentrations of BPS-10 (a) 40, (b) 60, and (c) 80 wt % in EAN and (d) 60 wt % in [Bmim]BF_4.

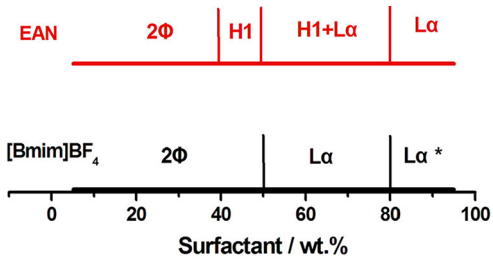

Figure 6. Phase diagrams for BPS-10 in binary systems with EAN and [Bmim]BF_4 at 25 °C. 2Φ, H1, and Lα indicate, respectively, two-phase coexistence, hexagonal, and lamellar phases.

solvophobic self-assembly process.[17] As a protic IL, EAN can form stronger hydrogen-bonded networks of EAN−EAN and $CH_3CH_2NH_3^+$−PEO than [Bmim]BF_4, which may promote LLC formation in EAN. This phenomenon can be also reasonably explained by the Gordon parameter,[8,30] which gives a measure of the cohesive energy density of the solvent. The higher Gordon parameter value of EAN indicates the stronger driving force for the self-assembly process.

The missing H1 phase in [Bmim]BF_4 could be attributed to the weaker driving force for the self-assembly process in [Bmim]BF_4 than that in EAN.[8] Such an effect may be explained more clearly by using the critical packing parameter (CPP), a powerful and simple tool to interpret the possible self-assembled structures. CPP is defined as $v/(a_0 l_c)$, where v, a_0, and l_c are the average volume of the surfactant, the effective head group area, and the effective length in the molten state, respectively.[31] Generally, the relationships between the self-assembly aggregates and CPP are usually shown as follows: the spherical micelles for CPP < 1/3, the rod-shaped micelles for 1/3 < CPP < 1/2, the bilayers and vesicles for 1/2 < CPP < 1, and the reverse structures when CPP > 1. For two BPS-10/IL systems, the v and l_c have basically the same values due to the rigidity of the steroid group, and only the a_0 shows a big difference. As seen in Table 1, the A_{min} value of BPS-10 in EAN is 0.50 nm^2, much larger than 0.27 nm^2 in [Bmim]BF_4. Take a_0 values similar to A_{min}, a lower CPP value in [Bmim]BF_4 than that in EAN is obvious, leading to the missing H1 phase.

Rheological Behavior. More information on the hydrogen-bonded network structure and the macro properties of the LLC phase at different ILs can be investigated from rheological experiments. As shown in Figure 7, the measured relationship

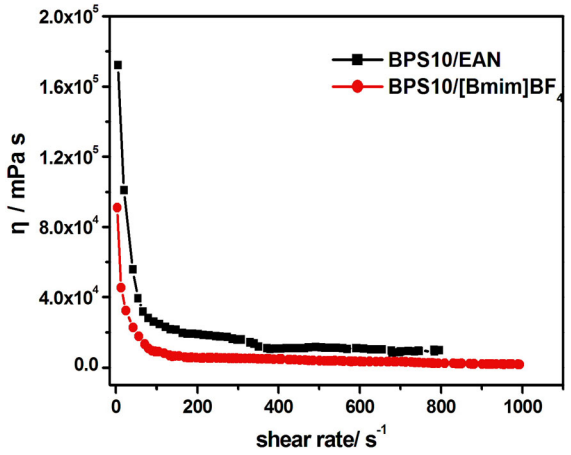

Figure 7. Flow curves for samples of 80% concentration BPS-10 in ILs at 25 °C.

of apparent viscosity with shear rate presents the shear-thinning rheology behaviors for the LLC phase formed by BPS-10 in both ILs. At the low shear rate, the sample of the EAN system exhibits a higher apparent viscosity of nearly 180000 mPa·s compared to the [Bmim]BF_4 system, which may be attributed to the stronger hydrogen-bonded networks. The results from the dynamic oscillatory measurements of two samples also indicate the different viscoelastic properties of Lα phases formed by BPS-10 in EAN and [Bmim]BF_4. As shown in Figure 8, both the storage (G') and the loss (G'') moduli of two Lα phase samples are large and increase with the sweep frequency, indicating a viscoelastic liquid character.[32] In the [Bmim]BF_4 system, G' is lower than G'' in a large measured frequency range, and the intersection of them can only be observed at a high frequency, exhibiting a very short stress

dx.doi.org/10.1021/jp305230r | J. Phys. Chem. B 2012, 116, 9439−9444

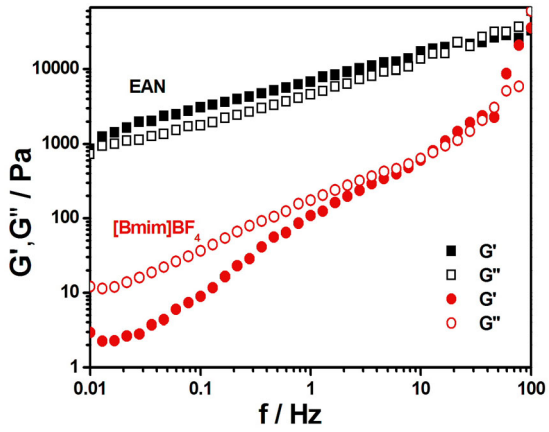

Figure 8. Variation of storage and loss moduli as a function of shear frequency, respectively, for an 80% concentration of BPS-10 in EAN (squares) and $[Bmim]BF_4$ (circles) at 25 °C.

relaxation time. However, the observed $G' > G''$ for the sample in EAN reflects an elastic behavior at the large measured frequency range. Moreover, the modulus values for the sample in EAN are much higher than those in $[Bmim]BF_4$. All of these results indicate that the Lα phase in EAN is highly viscoelastic with a high apparent viscosity, which also indicates the difference between EAN and $[Bmim]BF_4$.

CONCLUSIONS

The self-assemblies of nonionic surfactants in ionic liquids are driven by the solvophobic interaction combined with the hydrogen bonding. The protic IL could donate or accept protons to form hydrogen bonding, which is the origin to exhibit different solvophobic interactions and hydrogen bonding capabilities compared to those of the aprotic IL. Thus, the ethoxylated phytosterol surfactant does not show the same aggregation behaviors in ionic liquid solvents of protic EAN and aprotic $[Bmim]BF_4$. Due to the stronger solvophobic interaction, the micelles are more favorably formed and have much smaller size in EAN than those in $[Bmim]BF_4$. The ordered phase regions in EAN are expanded to lower BPS-10 concentrations compared to those in $[Bmim]BF_4$, suggesting a stronger self-assembly driving force in EAN. Moreover, the H1 phase observed in EAN but missing in $[Bmim]BF_4$ is attributed to the hydrogen-bonded network capability and higher Gordon parameter value of EAN. These facts clearly indicate that the protonation ability of EAN provides it an extra force to drive the surfactant molecules to form ordered aggregates. However, the generality of such a deduction needs to be verified for more systems. The obtained results should be a useful supplement to the aggregations of steroid surfactants in ionic liquid solvents.

AUTHOR INFORMATION

Corresponding Author

*E-mail: xchen@sdu.edu.cn. Tel: +86-531-88365420. Fax: +86-531-88564464.

Notes

The authors declare no competing financial interest.

ACKNOWLEDGMENTS

We are thankful for the financial support from the National Natural Science Foundation of China (20773080, 20973104, and 21033005) and Shandong Provincial Science Fund (2009ZRB01147).

REFERENCES

(1) Ma, Z.; Yu, J.; Dai, S. *Adv. Mater.* **2010**, *22*, 261−285.
(2) Zhao, D. B.; Wu, M.; Kou, Y.; Min, E. *Catal. Today* **2002**, *74*, 157−189.
(3) Lee, J. W.; Shin, J. Y.; Chun, Y. S.; Jang, H. B.; Song, C. E.; Sang-gi, L. *Acc. Chem. Res.* **2010**, *43*, 985−994.
(4) Pârvulescu, V. I.; Hardacre, C. *Chem. Rev.* **2007**, *107*, 2615−2665.
(5) Lagrost, C.; Carrie, D.; Vaultier, M.; Hapiot, P. *J. Phys. Chem. A* **2003**, *107*, 745−752.
(6) Buzzeo, M. C.; Evans, R. G.; Compton, R. G. *ChemPhysChem* **2004**, *5*, 1106−1120.
(7) Hao, J. C.; Zemb, T. *Curr. Opin. Colloid Interface Sci.* **2007**, *12*, 129−137.
(8) Greaves, T. L.; Drummond, C. J. *Chem. Soc. Rev.* **2008**, *37*, 1709−1726.
(9) Greaves, T. L.; Drummond, C. J. *Chem. Rev.* **2008**, *108*, 206−237.
(10) Patrascu, C.; Gauffre, F.; Nallet, F.; Bordes, R.; Oberdisse, J.; de Lauth-Viguerie, N.; Mingotaud, C. *ChemPhysChem* **2006**, *7*, 99−101.
(11) Inoue, T. *J. Colloid Interface Sci.* **2009**, *337*, 240−246.
(12) Inoue, T.; Yamakawa, H. *J. Colloid Interface Sci.* **2011**, *356*, 798−802.
(13) Araos, M. U.; Warr, G. G. *J. Phys. Chem. B* **2005**, *109*, 14275−14277.
(14) Araos, M. U.; Warr, G. G. *Langmuir* **2008**, *24*, 9354−9360.
(15) Atkin, R.; Warr, G. G. *J. Phys. Chem. B* **2007**, *111*, 9309−9316.
(16) Atkin, R.; Bobillier, S. M.; Warr, G. G. *J. Phys. Chem. B* **2010**, *114*, 1350−1360.
(17) Ma, F. M.; Chen, X.; Zhao, Y. R.; Wang, X. D.; Li, Q. H.; Lv, C.; Yue, X. *Langmuir* **2010**, *26*, 7802−7807.
(18) Zhang, G. D.; Chen, X.; Zhao, Y. R.; Ma, F. M.; Jing, B.; Qiu, H. Y. *J. Phys. Chem. B* **2008**, *112*, 6578−6584.
(19) Wang, L. Y.; Chen, X.; Chai, Y. C.; Hao, J. C.; Sui, Z. M.; Zhuang, W. C.; Sun, Z. W. *Chem. Commun.* **2004**, *24*, 2840−2841.
(20) Folmer, B. M.; Svensson, M.; Holmberg, K.; Brown, W. *J. Colloid Interface Sci.* **1999**, *213*, 112−120.
(21) Sakai, H.; Saitoh, T.; Endo, T.; Tsuchiya, K.; Sakai, K.; Abe, M. *Langmuir* **2009**, *25*, 2601−2603.
(22) Yue, X.; Chen, X.; Wang, X. D.; Li, Z. H. *Colloids Surf., A* **2011**, *392*, 225−232.
(23) Evans, D. F.; Yamauchi, A.; Roman, R.; Casassa, E. Z. *J. Colloid Interface Sci.* **1982**, *88*, 89−96.
(24) Evans, D. F.; Kaler, E. W.; Benton, W. J. *J. Phys. Chem. B* **1983**, *83*, 533−535.
(25) Zhao, G. X.; Zhu, B. Y. *Principles of surfactant action*; China Light Industry Press: Beijing, China, 2003; p 126.
(26) Sarkar, B.; Alexandridis, P. *J. Phys. Chem. B* **2010**, *114*, 4485−4494.
(27) Holmberg, K.; Jönsson, B.; Kronberg, B.; Lindman, B. In *Surfactants and Polymers in Aqueous Solution*, 2nd ed.; John Wiley & Sons: Chichester, U.K., 2002; p 54.
(28) Li, N.; Zhang, S. H.; Zheng, L. Q.; Inoue, T. *Langmuir* **2009**, *25*, 10473−10482.
(29) Greaves, T. L.; Mudie, S. T.; Drummond, C. J. *Phys. Chem. Chem. Phys.* **2011**, *13*, 20441−20452.
(30) Evans, D. F. Self-organization of amphiphiles. *Langmuir* **1988**, *4*, 3−12.
(31) Mitchell, D. J.; Ninham, B. W. *J. Chem. Soc., Faraday Trans.* **1981**, *77*, 601−629.
(32) Dürrschmidt, T.; Hoffmann, H. *Colloid Polym. Sci.* **2001**, *279*, 1005−1012.